Acta Crystallographica Section D
**Biological Crystallography**
ISSN 0907-4449

# Participation of Cys123$\alpha$ of *Escherichia coli* succinyl-CoA synthetase in catalysis

**Esther Hidber,[a] Edward R. Brownie,[b] Koto Hayakawa[b] and Marie E. Fraser[b]***

[a]Department of Biochemistry, University of Western Ontario, London, Ontario N6A 5C1, Canada, and [b]Department of Biological Sciences, University of Calgary, Calgary, Alberta T2N 1N4, Canada

Correspondence e-mail: frasm@ucalgary.ca

Received 26 April 2007
Accepted 14 June 2007

**PDB References:** succinyl-CoA synthetase, C123$\alpha$A mutant, 2nu6, r2nu6sf; C123$\alpha$S mutant, 2nu7, r2nu7sf; C123$\alpha$T mutant, tetragonal, 2nu8, r2nu8sf; C123$\alpha$T mutant, orthorhombic, 2nu9, r2nu96sf; C123$\alpha$V mutant, 2nua, r2nuasf.

Succinyl-CoA synthetase has a highly conserved cysteine residue, Cys123$\alpha$ in the *Escherichia coli* enzyme, that is located near the CoA-binding site and the active-site histidine residue. To test whether the succinyl moiety of succinyl-CoA is transferred to the thiol of Cys123$\alpha$ as part of the catalytic mechanism, this residue was mutated to alanine, serine, threonine and valine. Each mutant protein was catalytically active, although less active than the wild type. This proved that the specific formation of a thioester bond with Cys123$\alpha$ is not part of the catalytic mechanism. To understand why the mutations affected catalysis, the crystal structures of the four mutant proteins were determined. The alanine mutant showed no structural changes yet had reduced activity, suggesting that the size of the cysteine is important for optimal activity. These results explain why this cysteine residue is conserved in the sequences of succinyl-CoA synthetases from different sources.

## 1. Introduction

The enzyme succinyl-CoA synthetase (SCS) catalyzes the reversible reaction

$$\text{succinyl-CoA} + \text{NDP} + \text{P}_\text{i} \longleftrightarrow \text{succinate} + \text{CoA} + \text{NTP},$$

where N denotes adenosine or guanosine (Bridger, 1974; Nishimura, 1986). SCS consists of two different subunits designated $\alpha$ and $\beta$. CoA binds to the $\alpha$-subunit (Wolodko *et al.*, 1994), while the nucleotide binds to the amino-terminal domain of the $\beta$-subunit more than 30 Å away (Joyce *et al.*, 1999, 2000). The active-site histidine residue, His246$\alpha$[1] in *Escherichia coli* SCS, is transiently phosphorylated during the reaction. This histidine residue is thought to shuttle the phosphoryl group between the CoA-binding site and the nucleotide-binding site (Fraser *et al.*, 1999). In all structures of succinyl-CoA synthetase determined to date, the phosphohistidine or the histidine residue is bound near the free thiol group of CoA at the interface between the $\alpha$-subunit and the carboxy-terminal domain of the $\beta$-subunit (Wolodko *et al.*, 1994; Joyce *et al.*, 2000; Fraser *et al.*, 2000, 2002, 2006). The binding site for succinate or for the succinyl moiety of succinyl-CoA is thought to lie nearby, but has yet to be identified.

A cysteine residue, Cys123$\alpha$, lies near the free thiol group of CoA. In the structure of the wild-type enzyme the side chain

[1] Amino-acid residues in SCS are specified by the three-letter code followed by the residue number and either $\alpha$ or $\beta$ to indicate the subunit.

of Cys123$\alpha$ packs into the protein, but in the structure of the E197$\beta$A[2] mutant the side chain of Cys123$\alpha$ is exposed (Fraser *et al.*, 2002). This difference in conformation was unexpected, since the mutation E197$\beta$A is located $\sim$30 Å away from Cys123$\alpha$. The mutation was designed to disrupt the transfer of the phosphoryl group from NTP to the active-site histidine residue. It was postulated that this glutamate residue would accept a hydrogen bond from the imidazole ring when His246$\alpha$ was poised at the nucleotide-binding site. The E197$\beta$A mutant protein could not be phosphorylated by NTP, as had been expected. However, the fact that it could not be phosphorylated by succinyl-CoA and inorganic phosphate was a surprise. In the structure, the exposed side chain of Cys123$\alpha$ disrupted the binding of the free thiol end of CoA. It was postulated that in this conformation Cys123$\alpha$ would prevent the binding of the succinyl moiety of succinyl-CoA at the active site and that this was why the enzyme could not be phosphorylated by succinyl-CoA and inorganic phosphate.

Cys123$\alpha$ might be a catalytic residue, given the reactivity of the cysteine side chain and its location near CoA and the active-site histidine residue. One possibility is that the succinyl moiety is transferred from succinyl-CoA to Cys123$\alpha$, forming a thioester bond on the enzyme. Such a mechanism was proposed for the histone acetyltransferase yeast ESA1, where the acetyl group of acetyl-CoA was thought to be transferred to Cys304 of yeast ESA1 as part of the catalytic mechanism (Yan *et al.*, 2002). This mechanism was controversial, and further analysis, which included the mutation of this residue to alanine, showed that Cys304 was not an essential residue (Berndsen *et al.*, 2007). To test the possibility that the succinyl group of succinyl-CoA is transferred to Cys123$\alpha$ in *E. coli* SCS, this cysteine residue was mutated. In this work mutations to alanine, serine, threonine and valine were chosen because none of these mutants would be able to substitute for the cysteine residue in the catalytic reaction if a thioester bond had to be formed. The residues alanine and serine should be able to adopt either of the two conformations seen for Cys123$\alpha$, although the potential for serine to form hydrogen bonds might affect the equilibrium between the two conformations. Threonine and valine, two $\beta$-branched amino-acid residues, might have more difficulty packing into the protein, in part because of their size, but also because the conformation of the backbone is not ideal for $\beta$-branched amino-acid residues (Fersht, 1999; Leach *et al.*, 1966). If these mutations had no effect on catalysis, this would suggest that Cys123$\alpha$ plays no role in the catalytic mechanism. If instead the mutations led to a reduction of the catalytic efficiency but the mutant proteins were still active enzymes, the catalytic constants for the substrates could be determined in order to judge the effects of the mutations on the binding of substrates. When these experiments were performed, it was demonstrated that the mutant proteins were active enzymes but that they were less active than wild-type SCS. As a result, the mutant proteins were crystallized so that their structures could be determined using X-ray diffraction to aid in the interpretation of the kinetic data.

[2] Mutations are indicated by $X\#\alpha/\beta Y$, where $X$ is the single-letter code for the residue in the wild-type enzyme, # is the residue number, $\alpha$ or $\beta$ identifies the subunit and $Y$ is the residue type in the mutant protein.

## 2. Materials and methods

### 2.1. Construction, expression and purification of the site-directed mutants

The four mutations were made in the expression plasmid for *E. coli* SCS, pGS202 (Buck & Guest, 1989), using the QuikChange procedure. This plasmid contains both of the genes that encode succinyl-CoA synthetase, with the gene for the $\beta$-subunit located upstream of the gene for the $\alpha$-subunit as in *E. coli*. The mutagenic primers were 5′-CGTATGATCGGCCCGAAC**GCC**CCAGGCGTTATCACTCC-3′ and its complement for the C123$\alpha$A mutant. The codon for the mutation is highlighted in bold. The mutagenic primers for the other mutations were identical, except for the codons for the mutations: 5′-TCC-3′ and 5′-GGA-3′ for the C123$\alpha$S mutant, 5′-ACC-3′ and 5′-GGT-3′ for the C123$\alpha$T mutant and 5′-GTC-3′ and 5′-GAC-3′ for the C123$\alpha$V mutant. There was one change from the standard QuikChange protocol. To reduce the formation of primer dimers, the two primers for each mutant were added separately to two aliquots of plasmid and extended using the polymerase before combining the samples and proceeding with the standard protocol (Wang & Malcolm, 1999). For each mutation, the sequence of the portion of the plasmid encoding the protein was verified at the DNA Sequencing Facility, Robarts Research Institute, London, Ontario, Canada.

Each of the mutant plasmids was transformed into the *E. coli* SCS null strain TK3D18 ($\Delta$[kdp-suc]$\Delta$[gal-bio]; Rhodes *et al.*, 1978) for protein expression. This strain was grown using modified Luria–Bertani medium in which sodium chloride was replaced by potassium chloride and potassium glutamate (Buck & Guest, 1989). The modified medium contains 10 g tryptone, 5 g yeast extract, 10 g potassium chloride and 8.5 g potassium glutamate per litre and was adjusted to pH 7. To select for *E. coli* containing the plasmid, ampicillin was added to a concentration of 0.05 mg ml$^{-1}$. 100 ml of culture was grown overnight and then diluted 1:100 with fresh medium and 1 l cultures were grown in 2.8 l Fernbach flasks at 303 K. Once the optical density of the culture measured at 600 nm had reached 0.5, expression was induced by increasing the temperature to 315 K. The cultures were grown for 8 h at 315 K and the cells were then collected by centrifugation at 277 K. Following freezing at 193 K, the cells were sonicated in lysis buffer and the mutant proteins were purified using previously described methods (Wolodko *et al.*, 1986, 1994). The mutant proteins were stored at 277 K as precipitate suspensions by adding 50 g ammonium sulfate per 100 ml protein solution. The yield of purified protein ranged from 10 to 20 mg per litre of culture.

**Table 1**
Crystallization conditions for the mutant proteins.

| Mutant, space group | Protein solution | Well solution | Ratio of initial volumes, protein solution:well solution |
|---|---|---|---|
| C123$\alpha$A, $P4_322$ | 9.9 mg ml$^{-1}$ protein, 0.5 m*M* CoA | 100 m*M* Bicine pH 7.6, 2.10 *M* $(NH_4)_2SO_4$ | 2:1 |
| C123$\alpha$S, $P4_322$ | 8.7 mg ml$^{-1}$ protein, 0.5 m*M* CoA | 100 m*M* Bicine pH 7.6, 1.98 *M* $(NH_4)_2SO_4$ | 2:1 |
| C123$\alpha$T, $P4_322$ | 13 mg ml$^{-1}$ protein, 5 m*M* succinyl-CoA, 0.1 m*M* EDTA, 0.5 m*M* DTT | 100 m*M* Bicine pH 7.9, 1.86 *M* $(NH_4)_2SO_4$ | 1:1 |
| C123$\alpha$T, $P2_12_12_1$ | 12 mg ml$^{-1}$ protein, 0.5 m*M* CoA | 100 m*M* Bicine pH 8.0, 2.10 *M* $(NH_4)_2SO_4$ | 1:1 |
| C123$\alpha$V, *C*2 | 11 mg ml$^{-1}$ protein, 0.5 m*M* CoA | 91 m*M* MOPS pH 7.3, 1.45 *M* $(NH_4)_2SO_4$ | 1:1 |
| C123$\alpha$V, $P4_322$ | 10 mg ml$^{-1}$ protein, 5 m*M* CoA | 100 m*M* Tris–HCl pH 7.2, 2.00 *M* $(NH_4)_2SO_4$ | 1:1 |

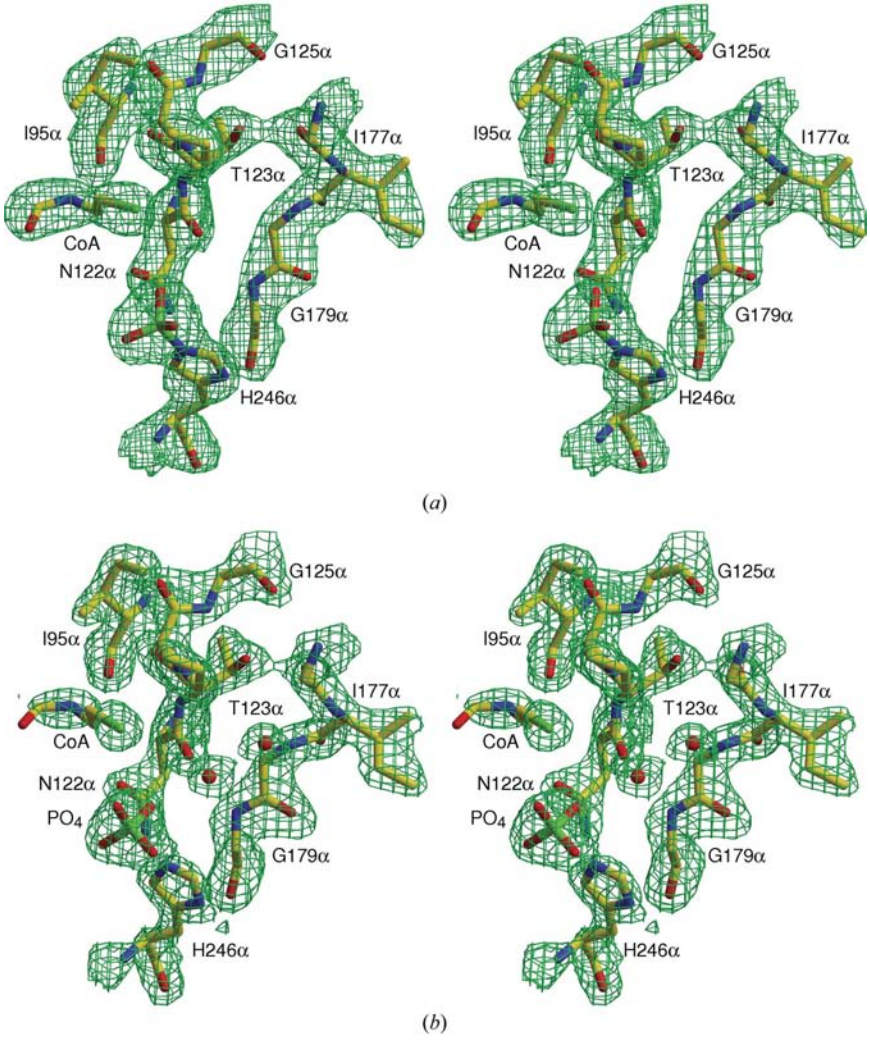


**Figure 1**
Stereoview of the electron density in the vicinity of the mutation for the C123$\alpha$T mutant. The model is represented by sticks with colours indicating the atom type: yellow, carbon; blue, nitrogen; red, oxygen; green, sulfur or phosphorus. The electron density is from the $2F_o - F_c$, $\alpha_c$ $\sigma_A$-weighted map (Read, 1986). The figure was drawn using the programs *XFIT* (McRee, 1999) and *RASTER3D* (Merritt & Bacon, 1997). (*a*) Orthorhombic crystal form, 2.9 Å resolution data contoured at 1.5$\sigma$. (*b*) Tetragonal crystal form, 2.15 Å resolution data contoured at 2$\sigma$.

### 2.2. Kinetic analyses of the C123$\alpha$A, C123$\alpha$S, C123$\alpha$T and C123$\alpha$V mutant proteins

Steady-state kinetic analyses of all four mutant proteins were performed as described for wild-type SCS (Joyce *et al.*, 1999) or other enzymatically active mutants (Joyce *et al.*, 1999; Fraser *et al.*, 2002). The concentrations of the mutant proteins were determined using the extinction coefficient at 280 nm determined for wild-type SCS, $E^{1\%}_{1\,cm}$ = 5.0 (Krebs & Bridger, 1974). Initial velocities were measured in triplicate at 294 K by following the production of succinyl-CoA spectrophotometrically at 235 nm using various concentrations of CoA, succinate or ATP with constant concentrations of the other substrates (129 m*M* CoA, 10 m*M* succinate and 441 m*M* ATP, as appropriate) in a 1 ml volume of 50 m*M* potassium chloride, 10 m*M* magnesium chloride and 50 m*M* Tris–HCl pH 7.4. The data were analyzed by nonlinear regression using the program *ENZYME KINETICS* v.1.5 (Stanislawski, 1991).

### 2.3. Crystallographic analyses of the C123$\alpha$A, C123$\alpha$S, C123$\alpha$T and C123$\alpha$V mutant proteins

Crystals of the four mutant proteins in complex with CoA were grown in hanging drops by vapour diffusion, essentially as described for the E197$\beta$A mutant (Fraser *et al.*, 2002). For each mutant protein an aliquot of the ammonium sulfate suspension was collected by centrifugation at 277 K, dissolved in 50 m*M* potassium phosphate pH 7.4 and dialyzed against the same buffer to remove residual ammonium ions. Still at 277 K, the proteins were phosphorylated using 5 m*M* ATP and 50 m*M* $MgCl_2$ in 50 m*M* 4-morpholinepropanesulfonic acid (MOPS) pH 7.4 or 50 m*M* *N*,*N*-bis(2-hydroxyethyl)glycine (Bicine) pH 7.6. The protein solutions were then dialyzed against several changes of buffer, first 50 m*M* potassium phosphate pH 7.4 and then 50 m*M* Bicine pH 7.6. The crystallization experiments were set up by adding 2 µl well solution (typically 2 *M* ammonium sulfate, 100 m*M* Bicine pH 7.6) to 2 or 4 µl of the protein solution (typically 10 mg ml$^{-1}$) on a plastic cover slip and equilibrating the drop over 1 ml well solution at 294 K. The specific conditions used to grow the crystals used for

the data collection are listed in Table 1. The best diffracting crystals grew as square plates or cubes to sizes suitable for X-ray diffraction (100–300 μm in the widest dimension) over a period of weeks. For the C123$\alpha$T mutant, crystals also grew as needles of approximately 30 μm in diameter. These crystals nucleated and grew very quickly, within days of the experiment being set up, and belonged to the orthorhombic space group $P2_12_12_1$. Crystals of the C123$\alpha$V mutant protein grew under similar conditions to those used for the other mutant proteins (Table 1), but they only appeared after several months and belonged to a different space group, $C2$, with unit-cell parameters $a$ = 394, $b$ = 92, $c$ = 97 Å, $\alpha = \gamma = 90$, $\beta = 98^\circ$. Since the first of these crystals diffracted to only 3.25 Å resolution and contained four $\alpha$-subunits and four $\beta$-subunits in the asymmetric unit, they were pursued only to the stage of solving the structure and no further. Crystals of the C123$\alpha$V mutant protein were also grown in the usual space group, $P4_322$ (Wolodko *et al.*, 1984, 1994), by macroseeding using seeds of the other mutants to induce crystallization. Prior to data collection at 100 K, crystals were cryoprotected by gradually increasing the concentration of glycerol in artificial mother liquor to 20%(*v*/*v*). This artificial mother liquor contained 1.8 *M* ammonium sulfate, 100 m*M* Bicine pH 7.8 for the crystals of the C123$\alpha$A, C123$\alpha$S and C123$\alpha$T mutant proteins and 2.0 *M* ammonium sulfate, 100 m*M* MOPS pH 7.3 for the C123$\alpha$V crystal. The diffraction data used to solve the structures were collected at beamlines A1 and F1 of the Cornell High Energy Synchrotron Source from crystals of the C123$\alpha$A, C123$\alpha$S and C123$\alpha$T mutant proteins and at beamline 8.3.1 of the Advanced Light Source from a crystal of the C123$\alpha$V mutant protein. The data were processed using the *HKL* program package (Otwinowski & Minor, 1997).

**Table 2**
Kinetic parameters of wild-type succinyl-CoA synthetase and mutant proteins.

| Protein | Succinate $K_{m(app)}$ (m*M*) | CoA $K_{m(app)}$ (μ*M*) | ATP $K_{m(app)}$ (m*M*) | $k_{cat}$ ($min^{-1}$) |
|---|---|---|---|---|
| Wild type† | 0.25 | 4.0 | 0.070 | 2684 |
| C123$\alpha$A | 0.71 ± 0.07 | 17 ± 4 | 0.18 ± 0.02 | 2123 |
| C123$\alpha$S | 0.80 ± 0.05 | 11 ± 2 | 0.10 ± 0.01 | 1755 |
| C123$\alpha$T | 3.3 ± 0.2 | 29 ± 4 | 0.10 ± 0.01 | 1860 |
| C123$\alpha$V | 1.3 ± 0.1 | 20 ± 6 | 0.09 ± 0.01 | 918 |

† Data from Joyce *et al.* (1999).

**Table 3**
Statistics for the X-ray diffraction data sets and the refined models.

Values in parentheses are for the highest resolution shell.

| SCS mutant | C123$\alpha$A | C123$\alpha$S | C123$\alpha$T | C123$\alpha$T | C123$\alpha$V |
|---|---|---|---|---|---|
| Resolution range (Å) | 34.37–2.55 (2.59–2.55) | 23.45–2.20 (2.24–2.20) | 41.97–2.15 (2.19–2.15) | 20.11–2.90 (2.95–2.90) | 97.51–2.95 (3.00–2.95) |
| Space group | $P4_322$ | $P4_322$ | $P4_322$ | $P2_12_12_1$ | $P4_322$ |
| Unit-cell parameters (Å, °) | $a = b = 97.2$, $c = 386.6$, $\alpha = \beta = \gamma = 90$ | $a = b = 96.6$, $c = 386.8$, $\alpha = \beta = \gamma = 90$ | $a = b = 96.7$, $c = 385.9$, $\alpha = \beta = \gamma = 90$ | $a = 98.5$, $b = 154.9$, $c = 240.6$, $\alpha = \beta = \gamma = 90$ | $a = b = 97.5$, $c = 390.3$, $\alpha = \beta = \gamma = 90$ |
| No. of measurements | 247358 | 271722 | 302730 | 356600 | 124742 |
| No. of unique reflections | 56818 | 88752 | 94811 | 81001 | 37218 |
| $\langle I\rangle/\langle\sigma(I)\rangle$† | 9.8 (1.4) | 10.9 (1.2) | 7.7 (1.2) | 12.2 (2.2) | 15.2 (1.3) |
| $R_{merge}$‡ | 0.141 (0.291) | 0.110 (0.334) | 0.140 (0.186) | 0.1116 (0.444) | 0.067 (0.421) |
| Completeness (%) | 88.8 (72.8) | 89.9 (64.8) | 89.9 (51.7) | 98.3 (83.2) | 90.7 (77.3) |
| $R_{work}$§ [No. of data] | 0.196 [48548] | 0.201 [76117] | 0.209 [81721] | 0.229 [76818] | 0.224 [32963] |
| $R_{free}$¶ [No. of data] | 0.247 [6521] | 0.244 [9773] | 0.255 [10573] | 0.251 [4125] | 0.266 [4191] |
| No. of protein atoms†† | 10012 | 9997 | 9963 | 19811 | 9972 |
| No. of atoms in noncovalently bound CoA molecules | 96 | 96 | 96 | 192 | 96 |
| No. of atoms in phosphate ions | 0 | 10 | 10 | 0 | 10 |
| No. of atoms in sulfate ions | 20 | 20 | 20 | 40 | 20 |
| No. of atoms in glycerol molecules | 0 | 0 | 6 | 0 | 0 |
| No. of water molecules | 257 | 368 | 534 | 4 | 5 |
| R.m.s. deviations from ideal geometry | | | | | |
| Bond lengths (Å) | 0.02 | 0.018 | 0.017 | 0.008 | 0.008 |
| Bond angles (°) | 2.2 | 2.0 | 2.0 | 1.4 | 1.5 |
| No. of residues in various regions of the Ramachandran plot | | | | | |
| Most favoured | 1016 [91.2%] | 1046 [93.9%] | 1038 [93.2%] | 2052 [92.4%] | 956 [85.8%] |
| Additional allowed | 95 [8.5%] | 66 [5.9%] | 73 [6.6%] | 164 [7.4%] | 146 [13.1%] |
| Generously allowed | 1 [0.1%] | 0 | 1 [0.1%] | 0 | 8 [0.7%] |
| Disallowed | 2 [0.2%] | 2 [0.2%] | 2 [0.2%] | 4 [0.2%] | 4 [0.4%] |
| R.m.s. deviations in temperature factors (Å$^2$) | | | | | |
| Main-chain atoms | 1.2 | 1.3 | 1.3 | 1.0 | 1.1 |
| Side-chain atoms | 2.0 | 2.2 | 2.1 | 1.6 | 1.7 |
| Average temperature factor for protein atoms [range] (Å$^2$) | 46 [20–90] | 42 [19–89] | 35 [17–92] | 38 [12–18] | 66 [27–100] |
| Average temperature factor for atoms in ligands or ions [range] | 61 [39–108] | 58 [36–81] | 42 [26–79] | 47 [22–69] | 71 [50–100] |
| Average temperature factor for water molecules [range] | 37 [18–66] | 41 [21–65] | 36 [14–62] | 29 [22–41] | 42 [32–60] |

† $\langle I\rangle$ is the mean intensity for all reflections, $\langle\sigma(I)\rangle$ is the mean sigma for these reflections. ‡ $R_{merge} = (\sum\sum|I_i - \langle I\rangle|)/\sum\sum\langle I\rangle$, where $I_i$ is the intensity of an individual measurement of a reflection and $\langle I\rangle$ is the mean value for all equivalent measurements of this reflection. § $R$ factor = $\sum||F_o| - |F_c||/\sum|F_o|$. ¶ $R$ factor based on data excluded from the refinement (~5%). †† The residues modelled are 1–287 of the $\alpha$-subunits, 1–388 of the $\beta$-subunit chain $B$ and 1–385 of the $\beta$-subunit chain $E$.

The starting model for the refinements was the previously published structure of *E. coli* SCS collected from a single crystal at low temperature (Fraser *et al.*, 2002), identified as 1jkj in the Protein Data Bank (Berman *et al.*, 2000). Programs from the *CCP*4 suite were used to perform the majority of the crystallographic calculations (Collaborative Computational Project, Number 4, 1994). The refinements used the maximum-likelihood target in the program *CNS* (Brünger *et al.*, 1998) with noncrystallographic symmetry restraints; iterative steps of refinement and rebuilding of the model were performed using the programs *TOM* (Jones, 1985) or *XFIT* (McRee, 1999) and checks of the stereochemistry of the models used the programs *PROCHECK* (Laskowski *et al.*, 1993) and *WHATCHECK* (Hooft *et al.*, 1996). The programs *SPDBV* (Guex & Peitsch, 1997) and *O* (Jones *et al.*, 1991) were used to superimpose and visualize the models.

## 3. Results

Each of the mutant proteins was expressed and purified in an enzymatically active form. This proved that succinate is not covalently bound to the side chain of Cys123$\alpha$ as part of the catalytic mechanism. Although the mutations do not abolish catalysis, they do affect the specific activity and the catalytic constants (Table 2). The largest change is in $K_{m(app)}$ for succinate. For example, the value is more than tenfold larger for the C123$\alpha$T mutant protein than for wild-type SCS (0.25 m*M*; Joyce *et al.*, 1999). This suggests that succinate is less tightly bound for all four of the mutants. CoA also binds more weakly to the mutant proteins, although the differences here are smaller, with the maximum difference being sevenfold for the C123$\alpha$T mutant protein compared with wild-type SCS (4.0 $\mu$*M*; Joyce *et al.*, 1999). The more similar values of $K_{m(app)}$ for ATP compared with wild-type SCS (0.07 m*M*; Joyce *et al.*, 1999) are the expected results since the mutations are near the binding sites for succinate and CoA but not near the binding site for ATP. Although the free thiol of Cys123$\alpha$ is not essential for the transfer of succinate, some characteristic of this side chain, possibly simply its size, is important for optimal catalytic activity.

Since there were differences between the kinetic constants for the mutant proteins and those for wild-type SCS, each mutant was crystallized and the structures were determined using X-ray diffraction. Table 3 shows the statistics for each data set and for the refined models. Crystals of all four mutant proteins were grown in the tetragonal space group $P4_322$, which was the crystal form used to solve the structure of *E. coli* SCS (Wolodko *et al.*, 1994). The ~400 Å axis of these crystals presents problems in the data collection because it leads to overlap of reflections when the long axis is in the direction of the incident X-rays, particularly if the mosaicity of the crystals is greater than 0.3°. The crystals of the C123$\alpha$T mutant protein that grew as needles belong to the orthorhombic space group $P2_12_12_1$. The longest unit-cell parameter of 240.6 Å is more amenable to data collection, but these crystals diffract to lower resolution, presumably because of their size. While the crystals belonging to the tetragonal space group contain two $\alpha\beta$ dimers in the asymmetric unit, crystals belonging to the orthorhombic space group contain two $\alpha_2\beta_2$ tetramers in the asymmetric unit. The octamer formed is the same as that seen in the tetragonal crystal form, in which the $\alpha\beta$ dimers pack across the crystallographic twofold axis to form an octamer (Fraser *et al.*, 1999). The octamer is not physiologically relevant, but arises, at least in part, from interactions of bound CoA with a $\beta$-subunit that is not part of the physiologically relevant tetramer. Site-directed mutagenesis experiments proved that in the tetragonal crystal form the physiologically relevant tetramer is formed by $\alpha\beta$ dimers that pack across the crystallographic twofold axis (Bailey *et al.*, 1999). This information is relevant here, allowing the identification of the $\alpha\beta$ dimers that form the physiologically relevant tetramer. Fig. 1 shows sample electron density for both the orthorhombic and tetragonal crystal forms to demonstrate the quality of the data at the two different resolutions. The best diffracting crystal (2.15 Å) was of the C123$\alpha$T mutant protein, which was grown from a solution of succinyl-CoA with ethylenediaminetetraacetic acid (EDTA) and the reducing agent dithiothreitol (DTT) (Table 1). The crystallization experiment was set up in the hope of obtaining a complex with succinyl-CoA, but instead there is clear electron density for CoA bound to the enzyme (Fig. 1*b*). During the time required for crystallization, the succinyl-CoA was obviously hydrolyzed in solution to give succinate and CoA.

For each of the mutant proteins, the side chain of residue 123 of the $\alpha$-subunit is buried and the free thiol of CoA lies near the backbone atoms. The active-site histidine residue, His246$\alpha$, is phosphorylated in the orthorhombic form of the C123$\alpha$T mutant protein (Fig. 1*a*) and is predominantly in the

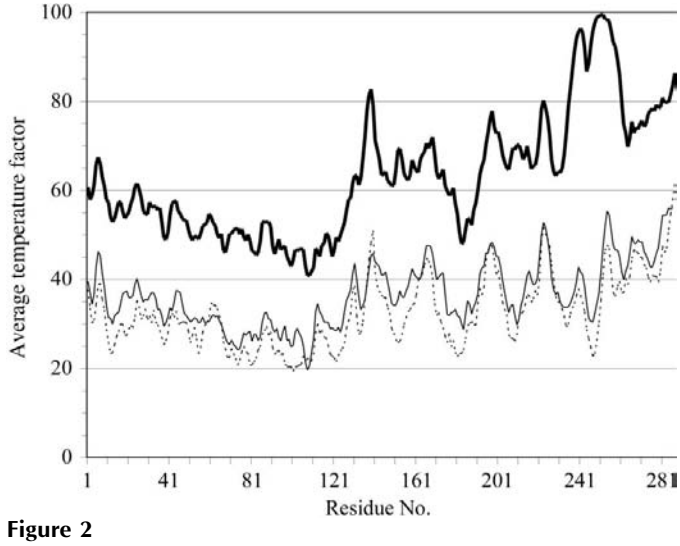


**Figure 2**
Plot of the temperature factors for main-chain atoms of the $\alpha$-subunit as a function of the residue number. The temperature factors were averaged over the copies of the $\alpha$-subunit in the asymmetric unit. The bold solid line represents averaged values for the C123$\alpha$V mutant protein, the dotted line represents wild-type *E. coli* SCS and the thin solid line represents the C123$\alpha$T mutant protein crystallized in the orthorhombic crystal form. Crystals of the C123$\alpha$V mutant protein and the C123$\alpha$T mutant protein diffract to similar resolutions, but the plot for the latter is more similar to that for wild-type *E. coli* SCS.

phosphorylated form in the C123$\alpha$A mutant protein. However, this residue is not phosphorylated in any of the other structures, including the C123$\alpha$T mutant protein in the tetragonal crystal form (Fig. 1*b*). Instead, there is an ion, modelled as phosphate, bound near the imidazole ring of His246$\alpha$ and interacting with residues of both the $\alpha$- and the $\beta$-subunits. Residues of the phosphohistidine loop in the C123$\alpha$V mutant protein are not well ordered, as is evident from the electron density (data not shown) and from a plot of the temperature factors of the backbone atoms (Fig. 2). The noncrystallographic symmetry was not imposed for residues between 237 and 257 of the $\alpha$-subunit in order to better model the disorder. The conformation of this loop is much better defined in each of the other mutants.

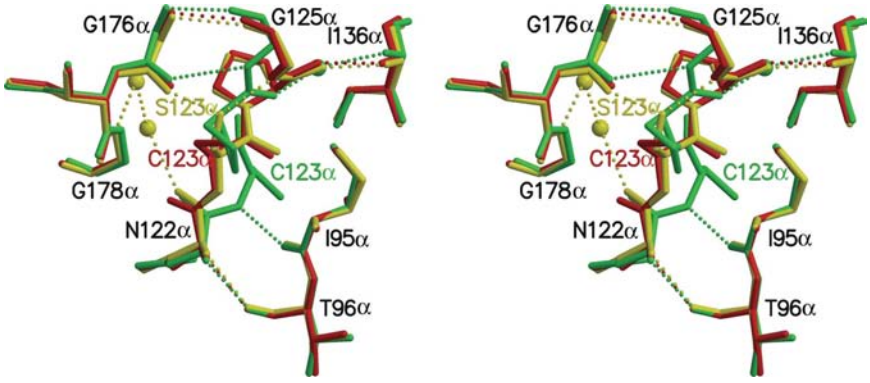


**Figure 3**
Stereoview of the superposition of structures of the C123$\alpha$S mutant protein, the E197$\beta$A mutant protein and wild-type *E. coli* SCS in the vicinity of residue 123 of the $\alpha$-subunit. The structures are shown as stick drawings shaded yellow, green and red, respectively. Dashed lines show important hydrogen-bonding interactions. This figure and Figs. 4 and 5 were drawn using the programs *MOLSCRIPT* (Kraulis, 1991) and *RASTER3D* (Merritt & Bacon, 1997).

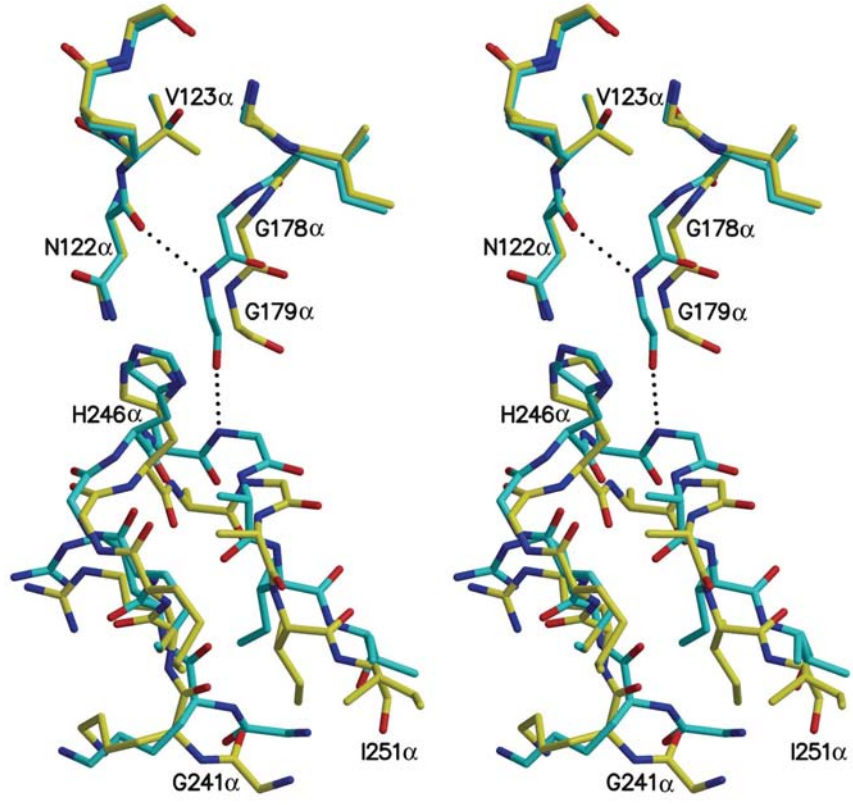


**Figure 4**
Stereoview showing part of the C123$\alpha$V mutant, including the phosphohistidine loop. For comparison, the model of the C123$\alpha$T mutant protein from the tetragonal crystal form is superposed. Shading is according to atom type, as in Fig. 1, but the C atoms for the C123$\alpha$T mutant are cyan. Dotted lines show hydrogen-bonding interactions present in the C123$\alpha$T mutant but not in the C123$\alpha$V mutant.

## 4. Discussion

The crystal structures prove that in every case the residue replacing Cys123$\alpha$ can pack into the protein. What these structures cannot show is whether this is the only conformation that the residue adopts during catalysis. If it is assumed that the residue also adopts the conformation seen in the crystal structure of the E197$\beta$A mutant protein, then the residue substituting for Cys123$\alpha$ must also be able to change conformation, flipping so that the side chain is exposed. When compared with wild-type SCS (Fraser *et al.*, 2002), there are no large differences between the conformations of the backbone atoms of the C123$\alpha$A, C123$\alpha$S or C123$\alpha$T mutant proteins in the vicinity of the mutation. More differences are seen for the C123$\alpha$V mutant protein and these differences will be discussed later in more detail. As an example, Fig. 3 shows the superposition of the structure of the C123$\alpha$S mutant protein in the vicinity of the substitution with the structures of the wild-type enzyme and the E197$\beta$A mutant protein (Fraser *et al.*, 2002). The $C^{\beta}$ atom of the serine residue and of each of the other residues substituted for Cys123$\alpha$ adopts a similar position to the $C^{\beta}$ atom of Cys123$\alpha$. In the C123$\alpha$A mutant protein, no changes result from the smaller size of the side chain; for example, there is no additional water molecule at the position of $S^{\gamma}$ of Cys123$\alpha$. In the C123$\alpha$S mutant protein, the new hydroxyl group forms hydrogen bonds to two main-chain atoms: the amide N atom of Gly125$\alpha$ (2.8 Å) and the carbonyl O atom of Gly176$\alpha$ (2.4 Å). This leads to a different position for $O^{\gamma}$ of Ser from that of $S^{\gamma}$ of Cys123$\alpha$. $O^{\gamma}$ is in a similar position to $C^{\beta}$ of Pro124$\alpha$ in the structure of the E197$\beta$A mutant protein, while $S^{\gamma}$ of Cys123$\alpha$ in wild-type SCS is in a similar position to $C^{\gamma}$ of the same proline residue. As in the case of the alanine mutant, there is no addition of a water molecule at the position of the $S^{\gamma}$ of Cys123$\alpha$. In the C123$\alpha$T mutant protein, the hydroxyl group forms similar hydrogen

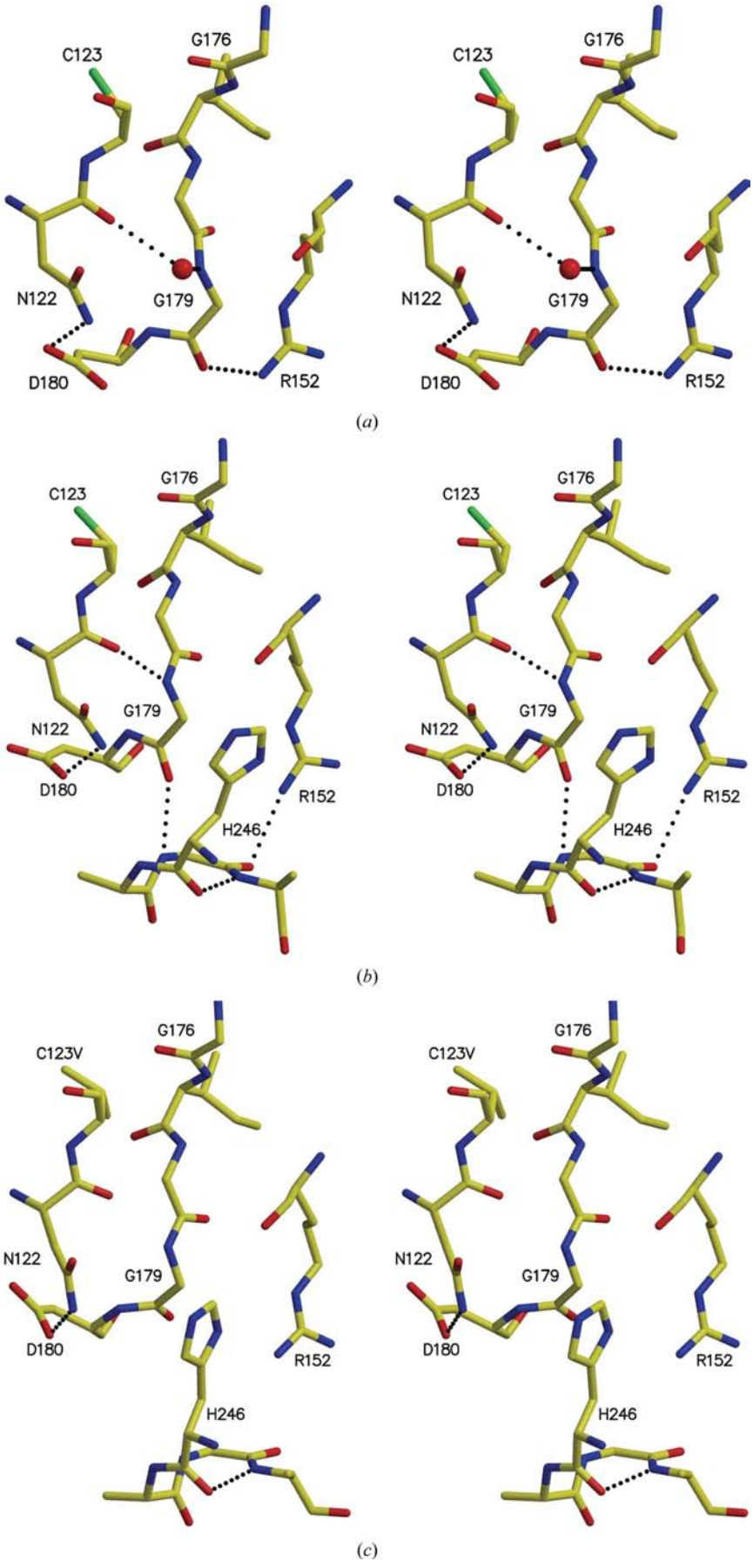


bonds to the C123$\alpha$S mutant, with lengths of 2.9 and 2.5 Å, respectively, while $C^{\gamma 2}$ adopts a similar position to that of $S^{\gamma}$ of Cys123$\alpha$. The conformational change anticipated from the structure of the E197$\beta$A mutant protein requires the residue at position 123$\alpha$ to flip, going from having a buried side chain to having this side chain exposed. It should be easier for alanine to change conformation than cysteine because of the smaller side chain of alanine. However, for serine or threonine to flip the hydrogen bonds with the backbone atoms would have to be broken, leading to greater activation energy for either of these changes than for Cys123$\alpha$.

In the crystal structures, most of the mutant proteins were dephosphorylated, despite the fact that the proteins had been phosphorylated prior to crystallization. The only protein that remained fully phosphorylated in the crystals was the C123$\alpha$T mutant, but only in the fast-growing orthorhombic crystal form. This suggests that (i) dephosphorylation occurred in solution prior to crystallization, since the slower growing crystals were dephosphorylated, and (ii) crystallization stabilized the phosphorylated histidine residue. The structure near the site of the mutation was similar in both the phosphorylated and dephosphorylated forms of the C123$\alpha$T mutant protein and we would expect the same to be true for the structures of the other mutant proteins. However, the mutations may destabilize the phosphorylated form.

The change from Cys123$\alpha$ to valine has the greatest effect on the structure. $C^{\gamma 2}$ of valine adopts a similar position to $S^{\gamma}$ of cysteine, leaving $C^{\gamma 1}$ to interact with the neighbouring strand at Gly178$\alpha$ (Fig. 4). The neighbouring strand from residue 178$\alpha$ to residue 181$\alpha$ has shifted away from the strand that includes residue 123$\alpha$, preventing a clash between $C^{\gamma 1}$ of Val123$\alpha$ and the N and $C^{\alpha}$ atoms of Gly178$\alpha$. At 3.8 Å, the distance between the carbonyl O atom

**Figure 5**
Stereoviews of the structures near residue 123 of the $\alpha$-subunit showing the effects of disorder of the phosphohistidine loop. The structures are shown as ball-and-stick drawings shaded according to atom type as in Fig. 1. Dashed lines show hydrogen-bonding interactions. (*a*) $\alpha$-Subunit of *T. thermophilus* SCS (PDB code 1oi7). (*b*) Wild-type *E. coli* SCS (Fraser *et al.*, 2002). (*c*) C123$\alpha$V mutant protein.

of Asn122$\alpha$ and the N atom of Gly179$\alpha$ is too long for a strong interaction. More importantly for the conformation of the phosphohistidine loop, the peptide between Gly179$\alpha$ and Asp180$\alpha$ adopts a different orientation from that in wild-type SCS, so that the carbonyl O atom is no longer in position to form a hydrogen bond to the N atom of Gly248$\alpha$. Although there are other shifts propagated through the C-terminal domain of the $\alpha$-subunit, this loss of a key hydrogen bond may lead to the disorder seen in the phosphohistidine loop of the C123$\alpha$V mutant protein.

The disorder seen in the phosphohistidine loop of the C123$\alpha$V mutant protein could emulate the movement that the phosphohistidine loop must make during catalysis in order to shift away from the CoA-binding site to the position where it interacts with the $\beta$-subunit and bound nucleotide. We would expect there to be conformational changes in residues of the $\alpha$-subunit, other than those of the phosphohistidine loop, to accommodate the conformational change. The flexibility of the protein that is seen in the vicinity of Gly179$\alpha$ accommodating the C123$\alpha$V mutation may be the same flexibility that is used in catalysis to allow the motion of the phosphohistidine loop. A second crystal structure, that of the $\alpha$-subunit of *Thermus thermophilus* SCS (PDB code 1oi7; H. Takahashi, Y. Tokunaga, C. Kuroishi, N. Babayeba, S. Kuramitsu, S. Yokoyama, M. Miyano & T. H. Tahirov, unpublished work), supports this interpretation. The structure of this $\alpha$-subunit was solved at very high resolution, 1.23 Å, but there is no electron density for residues of the phosphohistidine loop between residues 236$\alpha$ and 255$\alpha$. It appears that in the absence of the $\beta$-subunit the phosphohistidine loop does not adopt a single conformation. Since there are no interactions with the phosphohistidine loop, the structure of the rest of the $\alpha$-subunit of *T. thermophilus* SCS shows the conformation that it would adopt during the time that the phosphohistidine loop was moved away so that the active-site histidine could interact with the nucleotide. As in the structure of the C123$\alpha$V mutant protein, the carbonyl group of Gly179$\alpha$ of *T. thermophilus* SCS is rotated into the protein, in this case to form a hydrogen bond (3.0 Å) to the guanidinium group of Arg152 (Fig. 5*a*). This would compensate for the fact that the guanidinium group no longer has the carbonyl O atom of Gly248$\alpha$ of the phosphohistidine loop with which to interact. For reference, the structure of the same region of wild-type *E. coli* SCS is shown in Fig. 5(*b*). While in wild-type *E. coli* SCS the N atom of Gly179$\alpha$ donates a hydrogen bond to the carbonyl O atom of Asn122$\alpha$, the N atom of Gly179$\alpha$ of *T. thermophilus* SCS is too far from the carbonyl oxygen of Asn122$\alpha$ to form such a hydrogen bond (Fig. 5*a*). The same is true for the N atom of the equivalent residue of the C123$\alpha$V mutant protein (Fig. 5*c*). Instead, in the structure of the $\alpha$-subunit of *T. thermophilus* SCS (Fig. 5*a*), both the N atom of Gly179$\alpha$ and the carbonyl O atom of Asn122$\alpha$ are hydrogen bonded to a bridging water molecule. Although the resolution of the crystal structure for the C123$\alpha$V mutant protein is not sufficient to discern electron density for a similar bridging water molecule, the structures of the C123$\alpha$V mutant protein and the $\alpha$-subunit of *T. thermophilus* SCS are sufficiently similar near Gly179$\alpha$ to suggest that both possess the conformation adopted by the $\alpha$-subunit when the phosphohistidine loop has shifted away from the rest of the $\alpha$-subunit.

## 5. Conclusions

This work explains why the residue in the position equivalent to 123 of the $\alpha$-subunit of *E. coli* SCS is a highly conserved cysteine. The structure of the C123$\alpha$V mutant shows that a $\beta$-branched amino-acid residue disrupts the $\beta$-sheet in the $\alpha$-subunit. This leads to disorder in the phosphohistidine loop and, although we know that the phosphohistidine must be able to adopt the correct position for catalysis to occur since the mutant protein is an active enzyme, this conformation is not the one with lowest energy. The same disruption is likely to occur with longer residues, especially charged ones, even though they may not be $\beta$-branched. The C123$\alpha$T mutant is exceptional among the $\beta$-branched amino-acid residues because it forms a hydrogen bond to the neighbouring strand, allowing a closer interaction than would otherwise occur. The phosphohistidine loop is able to adopt the correct position for catalysis, but the mutation causes weaker binding of the substrates succinate and CoA and the mutant protein is a less efficient catalyst. A smaller side chain than cysteine does not disrupt the structure, but leads to lower catalytic efficiency, as in the C123$\alpha$A mutant protein. The structure of the C123$\alpha$A mutant protein does not show any reason for the lower catalytic efficiency, but the lower catalytic efficiency might be because the larger cysteine side chain is better at disrupting the binding of CoA or succinyl-CoA when the side chain is exposed, as seen in the E197$\beta$A mutant protein. We would hypothesize that the same results seen for the C123$\alpha$A mutant protein would be seen for the mutation to glycine. The C123$\alpha$S mutant protein has values for the binding constants that are most similar to the wild-type enzyme, but it is a less efficient catalyst because of its ability to form a hydrogen bond when buried. For catalytic efficiency, we would conclude that no naturally occurring amino-acid residue is able to substitute for Cys123$\alpha$.

The Natural Sciences and Engineering Research Council of Canada (NSERC) funded this work through a Discovery Grant and an Equipment Grant for computers. MEF was supported as an Alberta Heritage Foundation for Medical Research (AHFMR) Scholar. Crystallographic data were collected at the Cornell High Energy Synchrotron Source (CHESS) and the Advanced Light Source (ALS) at Lawrence Berkeley Laboratory. Research conducted at CHESS is supported by the National Science Foundation under award DMR-9311772, using the Macromolecular Diffraction at CHESS (MacCHESS) facility, which is supported by award RR-01646 from the National Institutes of Health Research. Data collected at the ALS were collected at beamline 8.3.1 under an agreement with the Alberta Synchrotron Institute (ASI). The ALS is operated by the Department of Energy and supported by the National Institutes of Health. Beamline 8.3.1

was funded by the National Science Foundation, the University of California and Henry Wheeler. The ASI synchrotron-access program is supported by grants from the Alberta Science and Research Authority and the AHFMR. We thank Dr William T. Wolodko for critically reading the manuscript.

## References

Bailey, D. L., Fraser, M. E., Bridger, W. A., James, M. N. G. & Wolodko, W. T. (1999). *J. Mol. Biol.* **285**, 1655–1666.
Berman, H. M., Westbrook, J., Feng, Z., Gilliland, G., Bhat, T. N., Weissig, H., Shindyalov, I. N. & Bourne, P. E. (2000). *Nucleic Acids Res.* **28**, 235–242.
Berndsen, C. E., Albaugh, B. N., Tan, S. & Denu, J. M. (2007). *Biochemistry*, **46**, 623–629.
Bridger, W. A. (1974). *The Enzymes*, edited by P. D. Boyer, Vol. 10, pp. 581–606. New York: Academic Press.
Brünger, A. T., Adams, P. D., Clore, G. M., DeLano, W. L., Gros, P., Grosse-Kunstleve, R. W., Jiang, J.-S., Kuszewski, J., Nilges, M., Pannu, N. S., Read, R. J., Rice, L. M., Simonson, T. & Warren, G. L. (1998). *Acta Cryst.* D**54**, 905–921.
Buck, D. & Guest, J. R. (1989). *Biochem. J.* **260**, 737–747.
Collaborative Computational Project, Number 4 (1994). *Acta Cryst.* D**50**, 760–763.
Fersht, A. (1999). *Structure and Mechanism in Protein Science: A Guide to Enzyme Catalysis and Protein Folding.* New York: W. H. Freeman.
Fraser, M. E., Hayakawa, K., Hume, M. S., Ryan, D. G. & Brownie, E. R. (2006). *J. Biol. Chem.* **281**, 11058–11065.
Fraser, M. E., James, M. N. G., Bridger, W. A. & Wolodko, W. T. (1999). *J. Mol. Biol.* **285**, 1633–1653.
Fraser, M. E., James, M. N. G., Bridger, W. A. & Wolodko, W. T. (2000). *J. Mol. Biol.* **299**, 1325–1339.
Fraser, M. E., Joyce, M. A., Ryan, D. G. & Wolodko, W. T. (2002). *Biochemistry*, **41**, 537–546.
Guex, N. & Peitsch, M. C. (1997). *Electrophoresis*, **18**, 2714–2723.
Hooft, R. W. W., Vriend, G., Sander, C. & Abola, E. E. (1996). *Nature (London)*, **381**, 272.
Jones, T. A. (1985). *Methods Enzymol.* **115**, 157–171.
Jones, T. A., Zou, J.-Y., Cowan, S. W. & Kjeldgaard, M. (1991). *Acta Cryst.* A**47**, 110–119.
Joyce, M. A., Fraser, M. E., Brownie, E. R., James, M. N. G., Bridger, W. A. & Wolodko, W. T. (1999). *Biochemistry*, **38**, 7273–7283.
Joyce, M. A., Fraser, M. E., James, M. N. G., Bridger, W. A. & Wolodko, W. T. (2000). *Biochemistry*, **39**, 17–25.
Kraulis, P. J. (1991). *J. Appl. Cryst.* **24**, 946–950.
Krebs, A. & Bridger, W. A. (1974). *Can. J. Biochem.* **52**, 594–598.
Laskowski, R. A., MacArthur, M. W., Moss, D. S. & Thornton, J. M. (1993). *J. Appl. Cryst.* **26**, 283–291.
Leach, S. J., Nemethy, G. & Scheraga, H. A. (1966). *Biopolymers*, **4**, 369–407.
McRee, D. E. (1999). *J. Struct. Biol.* **125**, 156–165.
Merritt, E. A. & Bacon, D. J. (1997). *Methods Enzymol.* **277**, 505–524.
Nishimura, J. S. (1986). *Adv. Enzymol. Relat. Areas Mol. Biol.* 141–172.
Otwinowski, Z. & Minor, W. (1997). *Methods Enzymol.* **276**, 307–326.
Read, R. J. (1986). *Acta Cryst.* A**42**, 140–149.
Rhodes, D. B., Laimins, L. & Epstein, W. (1978). *J. Bacteriol.* **135**, 445–452.
Stanislawski, J. (1991). *ENZYME KINETICS*, v.1.11. Trinity Software, Plymouth, NH, USA.
Wang, W. & Malcolm, B. A. (1999). *Biotechniques*, **26**, 680–682.
Wolodko, W. T., Fraser, M. E., James, M. N. G. & Bridger, W. A. (1994). *J. Biol. Chem.* **269**, 10883–10890.
Wolodko, W. T., James, M. N. G. & Bridger, W. A. (1984). *J. Biol. Chem.* **259**, 5316–5320.
Wolodko, W. T., Kay, C. M. & Bridger, W. A. (1986). *Biochemistry*, **25**, 5420–5425.
Yan, Y., Harper, S., Speicher, D. W. & Marmorstein, R. (2002). *Nature Struct. Biol.* **9**, 862–869.